Barbeiro Camila de Oliveira (Orcid ID: 0000-0002-8166-0101)

Title Page

High density of CD8 T cell and immune imbalance of T lymphocytes subsets are associated with proliferative verrucous leukoplakia

Darcy Fernandes[1#], Camila de Oliveira Barbeiro[1#], Mariana Paravani Palaçon[1], Mariel Ruivo Biancardi[1], Túlio Morandim Ferrisse[1], Heitor Albergoni Silveira[1], Rogerio Moraes Castilho[2], Luciana Yamamoto de Almeida[1], Jorge Esquiche Leon[3], Andreia Bufalino[1].

#: These authors contributed equally to this work and should be considered joint first authors.

[1]Oral Medicine, Department of Diagnosis and Surgery, São Paulo State University (Unesp), School of Dentistry, Araraquara, SP, Brazil.

[2]Laboratory of Epithelial Biology, Department of Periodontics and Oral Medicine, University of Michigan, School of Dentistry, Ann Arbor, MI, USA.

[3]Oral Pathology, Department of Stomatology, Public Oral Health and Forensic Dentistry, Ribeirão Preto Dental School, University of São Paulo (FORP/USP), Ribeirão Preto, SP, Brazil.

Corresponding author: Andreia Bufalino, Rua Humaitá, 1680, Araraquara, SP 14801-903, Brazil, TEL (+55) 016 3301-6382. E-mail: andreia.bufalino@unesp.br

Funding information

This study was financially supported by the São Paulo Research Foundation (FAPESP 2017/01438-0; 2017/01798-7; 2017/17288-8; 2018/22236-0; 2018/04954-2, #2021/01191-0; #2013/07276-1 [CePID CePOF]), Coordenação de Aperfeiçoamento de Pessoal de Nível Superior - Brasil (CAPES) – Finance code 001 and National Council for Scientific and Technological Development CNPq (423945/2016-5).

Compliance with Ethical Standards

Conflict of interest disclosure

The authors have no competing interests to declare.

Data Availability

The data that support the findings of this study are available on request from the corresponding author. The data are not publicly available due to privacy or ethical restrictions.

Ethical Approval

All samples used in this study were collected according to an institutional review board-approved clinical protocol after written informed consent was obtained (CAAE: 34361814.9.0000.5416).

Informed Consent

Informed consent was obtained from all participants included in the study.

ABSTRACT

Oral leukoplakia (OL) and proliferative verrucous leukoplakia (PVL) are oral potentially malignant disorders (OPMDs) that microscopically show no or varying degrees of dysplasia. Even sharing clinical and microscopic aspects, PVL shows a more aggressive clinical behavior, with a malignant transformation rate greater than 40%. Inflammatory infiltrate associated with dysplastic lesions may favor malignant transformation of OPMDs. This study aimed to evaluate the density of T cells and cytokines in dysplastic lesions from OL and PVL patients. Additionally, we evaluated whether soluble products produced in vitro by dysplastic keratinocytes are capable of modulating apoptosis rates and Th phenotype (Th1, Th2, Th17, and Treg) of peripheral blood mononuclear cells. The density of CD3, CD4, and CD8 T cells was assessed by immunohistochemistry. Cytokines and chemokines profile from frozen tissue samples were analyzed using the LUMINEX system. Apoptosis rates and Th phenotype modulation were evaluated by flow cytometry. Our results showed an increase in the number of CD8 Tcell in the subepithelial region from PVL dysplastic lesions in relation to OL samples. PVL showed increased levels of IL-5 and a decrease in IL-1β and IFN-γ levels compared to OL. Soluble products of PVL and oral carcinoma cell cultures were able to reduce apoptosis rate and promote an imbalance of Th1/Th2 and Th17/Treg. The high subepithelial density of CD8 T cells and immune imbalance of T lymphocytes subsets probably play an important role in the pathogenesis of PVL and may explain its more aggressive behavior in relation to OL.

Keywords: Epithelial dysplasia, Oral leukoplakia; Proliferative verrucous leukoplakia; malignant transformation; Lymphocytes.

Main Body

INTRODUCTION

Oral epithelial dysplasia is defined as a spectrum of architectural and cytological epithelial changes caused by the accumulation of genetic changes, associated with an increased risk of progression to squamous cell carcinoma.[1,2] Currently, it is well established that oral potentially malignant disorders (OPMD) with epithelial dysplasia are more often associated with malignant transformation to oral squamous cell carcinoma (OSCC).[1,3,4] Oral leukoplakia (OL), and proliferative verrucous leukoplakia (PVL) are examples of OPMD that microscopically reveal epithelial lesions without or with epithelial dysplasia and clinically present as a white plaque that may have different patterns including homogenous, verrucous/nodular, or erythroplakia. [2, 5,6,7]

OL has an incidence rate that varies from 1 to 4% and a recent systematic review showed a malignant transformation rate of around 9.8%.[1, 8, 9] The most affected sites are the vermilion of the lip, cheek mucosa, and gums, with men over the age of 40 being the most affected, although some studies show that there is no predilection for sex. [5, 10] The risk factors associated with OL are similar to those associated with OSCCs and include smoking, excessive alcohol consumption, old age, betel's knot, and exposure to ultraviolet radiation in cases that affect the vermilion lip.[11] On the other hand, PVL presents as a white plaque that tends to become multifocal with an aggressive, progressive, and irreversible behavior. [7, 11, 12] The rate of malignant transformation of PVL into OSCC or oral verrucous carcinoma varies from 14.3% to 75%, with an average rate ranging from 43.87% to 65.8%. [13,14] Unlike OL and OSCC, the etiology of PVL is not always associated with the risk factors, such as tobacco, alcohol, and areca. [7, 8, 11, 12,] The diagnosis of PVL is based on multiple periodic biopsies that may reveal different degrees of dysplasia or even the presence of OSCC. [11]

Although OL and PVL share some clinical and microscopic characteristics, it is well described that cellular and molecular differences favor malignant transformation in PVL. The OPMD microenvironment is usually composed of a chronic inflammatory infiltrate which has been described to play role in the process of malignant transformation. [8, 15,16] It is well known that the immune system may identify and destroy pre-neoplastic cells in a process called immunosurveillance, which works as an important defense against cancer. [16,17,18,19,20] Despite evidence in favor of the fundamental role of the immune system in eliminating cancer, it has been

shown that tumor cells can use the tumor's inflammatory infiltrate to progress through selection, subversion, and suppression of the immune system. [15, 16,17, 18, 19, 20, 21] However, the influence of inflammatory cells in OL and PVL behavior remains unknown. Thereby, we aimed to evaluate and compare the density of T helper cells (Th) and T cytotoxic cells (Tc), including related cytokines, in dysplastic lesions from OL and PVL patients. Additionally, we evaluated whether soluble products produced in vitro by dysplastic keratinocytes are capable of modulating apoptosis rates and the Th phenotype of peripheral blood mononuclear cells (PBMC).

MATERIALS AND METHODS

Patients and tissue collection

For this study 46 oral tissue specimens were provided by the Department of Diagnosis and Surgery, São Paulo State University (Unesp), School of Dentistry (Brazil). After performing the biopsy, the tissue specimens were divided into two parts of 10 mm each. One of the fragments was fixed in 4% paraformaldehyde and processed for histopathological and immunohistochemical analysis. The second part of the tissue specimens was immediately frozen in nitrogen and kept in a -80º freezer. All specimens included in this study microscopically revealed hyperkeratosis without or with oral epithelial dysplasia (mild, moderate, or severe) or verrucous hyperplasia, and they were collected from patients with a definitive clinicopathological diagnosis of OL or PVL established according to strict criteria.[1, 22, 23, 24, 25] Hematoxylin-eosin stained sections were used to assess the presence and degree of oral dysplasia by two experienced and independent pathologists (J.E.L. and H.A.S.), previously calibrated, following the WHO classification[1]. Subsequently, the samples were classified according to the potential susceptibility for malignant transformation into "low-risk" and "high-risk" lesions, according to the binary system proposed by Kujan et al., 2006.[23] In this system, Kujan et al. group in "low-risk" lesions those with less than four architectural changes or less than five cytological changes, and in the high-risk group are lesions that present at least four architectural changes and five cytological changes. These specimens were then divided into two groups. Group 1 was composed of 19 specimens of biopsies from 19 patients with a clinicopathological diagnosis of OL and an average follow-up period of six years, calculated from the time of the biopsy. Group 2 consisted of 27 specimens of biopsies from 12 patients with a clinicopathological diagnosis of PVL. This archive has an average follow-up period of seven years

and approximately two to three biopsies from each patient were collected from different oral sites, considering that PVL generally affects multiple sites. OL and PVL patients included in this study had a minimum follow-up of five years after the confirmation of the diagnosis.

In addition, to evaluate the profile of cytokines and chemokines through LUMINEX® system, 12 samples from OSCC patients and 14 non-neoplastic inflammatory reaction (inflammatory fibrous hyperplasia - IFH) samples obtained from healthy donors were included as control groups. For this type of assay, it is important to use control groups that allow the comparison of immunological profiles. All samples used in this study were collected according to an institutional review board-approved clinical protocol after written informed consent was obtained (CAAE: 34361814.9.0000.5416). All study subjects received written informed consent.

Immunohistochemical analysis

Oral tissue specimens were collected from OL and PVL patients as described above and fixed in 4% formalin and paraffin-embedded. The paraffin sections were dewaxed in xylol and rehydrated in a series of alcohols (95, 80, and 70%). Immunohistochemistry for cell typing was carried out using primary antibodies against CD3 and CD8 (#GA503 and #IR649, respectively, Dako, Carpinteria, CA, USA), and CD4 (CD4-368-L-CE, Leica Biosystems, Wetzlar, HE, Germany), followed by the LSAB method (#K0675, Dako, Carpinteria, CA, USA). After, the sections were incubated with 0.6mg/ml 3,3'diaminobenzidine tetrahydrochloride (DAB, Sigma-Aldrich, Saint Louis, MO, USA) and counterstained with Harris hematoxylin. Negative controls were obtained by suppressing the primary antibodies. Five representative fields were photographed separately from the intraepithelial and the subepithelial areas with an Olympus DP25 camera (Olympus, Center Valley, PA, USA) attached to the Nikon Eclipse E600 microscope (Nikon, Tokyo, Japan) utilizing a 20× objective. The positive cells were counted by two previously calibrated independent examiners using the Image J software (version 1.52, NIH, Bethesda, MD, USA). Quantification was performed by the average of the 5 fields.

Cytokines and Chemokines Assays

The profile of inflammatory cytokines from the frozen tissue samples was analyzed using the LUMINEX® system. Total proteins were extracted from frozen tissue samples using a detergent-based extraction buffer T-PER (Tissue Protein Extraction Reagent - Pierce, Rockford, IL, USA) containing a protease inhibitor cocktail (Complete Protease Inhibitor Cocktail Tablets; Roche Diagnostics, Indianapolis, IN, USA). A panel of 26 cytokines and chemokines, including GM-CSF, IFN-γ, IL-1β, IL-2, IL-4, IL-5, IL-6, IL-9, IL-10, IL-12p70, IL-13, IL-17A, IL-18, IL-21, IL-22, IL-23, IL-27, TNF-α, Granzyme A, Granzyme B, Perforin, MIP-1α, MIP-1β, sCD137, sFas, and sFasL, was used to assess CD4+ cell subsets (#EPX180-12165-901, ThermoFisher Scientific, Waltham, MA, USA), and the activation status of CD8+ cells (#HCD8MAG-15K, Merck Millipore Corporation, Billerica, MA, USA). Samples were processed following the manufacturer's instructions and then read on the Luminex's MAGPIX® instrument. Data analysis was performed using the xPONENT® software (Luminex Corporation, Austin, TX, USA).

Preparation of peripheral blood mononuclear cells (PBMC)

To obtain PBMC, peripheral blood was collected from the same healthy donor (without diabetes, hepatitis, and HIV) for all experiments. The technique of Ficoll–Hypaque density centrifugation of heparinized blood was used to obtain peripheral blood mononuclear cells (PBMC). The PBMC composite sediment was resuspended in RPMI 1640 culture medium (Invitrogen, USA) supplemented with L-Glutamine, 10% fetal bovine serum (FBS; Cultilab Ltda, Brazil), 10 mM HEPES (4-(2-hydroxyethyl)-1-piperazineethanesulfonic acid) and 200 U/ml of Penicillin/Streptomycin (Invitrogen, USA).

Primary Cell Cultures of Oral Keratinocytes and cell lines

We used primary cell culture derived from dysplastic oral keratinocytes from proliferative verrucous leukoplakia (DOK-PVL) and normal human oral keratinocytes (HOK). In order to obtain HOK, fragments of gingival tissue were collected from volunteer subjects who underwent clinical crown augmentation surgery. While DOK-PVL was obtained from a white lesion located on the lower alveolar ridge of a 76-year-old man and the degree of dysplasia, described as

mild/moderate, from a volunteer patient with a previous clinicopathological diagnosis of PVL. The protocol for the primary cell was based on a previous study.[25] The epithelial origin of the isolated cells was confirmed by immunofluorescence with antibody to human cytokeratin AE1/AE3 (Abcam, UK). Morphology and Immunofluorescence staining of DOK-PVL and HOK are presented in **Supplementary 1**.

In addition, the cell lines DOK and SCC-25 were used in this study, all obtained commercially. The human dysplastic keratinocyte cell line, DOK (CVCL_1180; ECACC - European Collection of Authenticated Cell Cultures, London, UK), comes from a white lesion on the back of the tongue of a 57-year-old man, and the degree of dysplasia has been described as mild/moderate. This cell line was cultivated in DMEM culture medium (Gibco) supplemented with L-Glutamine, 10% Fetal Bovine Serum (Lonza), 5 µg/mL hydrocortisone, and 200 U/mL Penicillin/Streptomycin (Gibco). The SCC-25 cell line (CRL-1628) comes from a human tongue SCC obtained from a 70-year-old man and was purchased from the American Type Culture Collection (ATCC, USA). These cells were grown in a culture medium composed of equal parts of DMEM and Ham's F12 medium (DMEM/F12; Invitrogen, USA) containing 1.2 g/L sodium bicarbonate, 2.5 mM L-glutamine, 15 mM HEPES and 0.5 mM sodium pyruvate supplemented with 10% FBS (Cultilab Ltds, Brazil), 0.4 µg/ml hydrocortisone (Sigma-Aldrich, USA) and antibiotic (Invitrogen, USA). All cell lines were kept at 37 ° C and 5% CO_2.

Conditioned Medium (CM)

CM was prepared using HOK, DOK, DOK-PVL, and SCC-25 cell cultures. Briefly, $1x10^6$ cells from each of the 4 cell types were cultivated on 100 mm^2 plates and maintained in culture until they reached approximately 80% confluence. RPMI 1640 culture medium (4 ml) was added to each plate, which was collected after 24 h and immediately aliquoted and kept in a -20C freezer until use. For carrying out the experiments, the PBMC were grown in the proportion of 1:1 (vol: vol) of CM and fresh unconditioned culture medium RPMI 1640. The unconditioned RPMI culture medium was used as a reference sample.

Immunophenotyping by Flow Cytometry

Two commercially available kits were used to characterize Th1, Th2, Th17, and Treg (# 560751 and # 560762; BD Biosciences, USA). The immunophenotyping kits used provided a cocktail of primary antibodies for the detection of human CD4, IFN-γ (for Th1), IL-4 (for Th2), IL-17A (for Th17), and FoxP3 (Treg). Briefly, PBMC were grown in RPMI 1640 or CM produced by different cell cultures (HOK, DOK, DOK-PVL, and SCC-25), both supplemented with 10% FBS, for a period of 72h at 37ºC and 5% CO_2. Monensin (10 µg/ml) was added for 4 hours before the end of the culture to ensure the retention of cytokines inside the cell. After incubation, approximately $3x10^6$ PBMC were collected and centrifuged at 500 g for 5 min. The cells were then washed in saline solution containing 1% FBS and 0.01% sodium azide (solution called stain buffer), centrifuged and then the PBMC were fixed according to the manufacturer guidelines. Then, the cells were incubated for 30 minutes, at room temperature, with each of the cocktails. After incubation, the cells were washed with stain buffer and centrifuged at 500 g for 5 minutes. All the analysis was made in a LSR Fortessa flow cytometer (BD Biosciences) and the data were analyzed using the FACSDiva software (version 8.0.1, BD Biosciences).

Analysis of Apoptosis Index in PBMC

To access the rates of cell death due to apoptosis, $3x10^5$ PBM were cultured in 12-well plates in the presence of MC from the HOK, DOK, DOK-PVL, and SCC-25 cell cultures or RPMI 1640 non-conditioned culture medium, in the times of 24 and 48h. After the previously determined periods, the cells were transferred to sterile tubes and centrifuged for 5 min at 400 g. The precipitated cells were resuspended in 100 µl of binding buffer (10 mM HEPES pH 7.4, 140 mM NaCl, and 2.5 mM CaCl2) containing 5 µl of annexin-V PE and 5 µl of 7-AAD (BD Pharmingen, USA). After incubation, 400 µl of binding buffer was added and the percentage of positive cells was determined by reading 10,000 events on a FACSVerse flow cytometer (BD Biosciences, USA), followed by analyzing the data in the FlowJo software (version 10.0.7, Tree Star).

Statistical analyses

The data were tabulated and the normal or non-normal distribution was determined by the Shapiro-Wilk normality test and by the descriptive analysis of skewness and kurtosis for subsequent application of adequate statistical tests according to the data distribution. For analysis of multiple comparisons within groups, analyses of variance (ANOVA ONE-WAY) and Kruskal Wallis were performed, according to the distribution of samples (normal or non-normal). In the presence of a statistically significant difference, the Tukey post-test and Dunn's post-test were performed, respectively. Additionally, Spearman's correlation test was used to determine the correlation between the density of CD4+ and CD8+ cells and the cytokine and chemokine levels of dysplastic lesions of OL and PVL groups. In addition, a simple linear correlation was performed to assess the correlation of effect and influence between each T cell marker (CD3, CD4, and CD8) for OL and PVL. Simple logistic regressions were performed to evaluate the predictive role of CD3+, CD4+ and CD8+ cells in the malignant transformation risk for OL and PVL. In this regard, the level of T cell markers was divided into high and low levels according to the mean. P-values <0.05 were considered significant and all the analyses were made in SPSS version 20.0 and the graphs were prepared using the Prism 8 GraphPad.

RESULTS

The density of CD8+ T cells is high in the subepithelial region of the dysplastic lesions in the PVL group

All the clinicopathological data of OL and PVL patients are shown in **Table 1**. Immunohistochemical staining for CD3 cells showed a membranous and/or cytoplasmic staining, while CD4 and CD8 cells showed limited staining to the superficial membrane. In addition, it was observed that in the connective tissue these T cells were observed as a sub-epithelial infiltrate in close relationship with the basal cell layer of the epithelium. When infiltrating the epithelial tissue, these cells were seen mainly in the basal and spinous layers of the epithelium of the two groups studied. In **Figure 1**, the tissue fragments are stained with hematoxylin and eosin (H&E), and the immunohistochemical staining pattern for CD3, CD4, and CD8 T lymphocytes in representative samples of the OL and PVL groups is shown.

Comparative analysis of the density of CD3, CD4, and CD8 T cells in the intraepithelial compartment of the OL and PVL groups did not reveal statistically significant differences between the groups. However, an increase in the number of CD3 (P = 0.001/Power = 0.928) and CD8 cells (P = 0.024/ Power = 0.972) (both $P<0.0001$) was observed in the subepithelial region of the dysplastic lesions in the PVL group in relation to samples from the OL group (**Figure 2**). Furthermore, after the logistic regression study, we have noted that for PVL, a high density of CD8+ cells is associated with high-risk dysplasia, being the odds ratio equal to 6.8571 ($P= 0.0452$) (**Table 2**).

Performing a simple linear regression analysis between the CD3, CD4, and CD8 markers in the two groups evaluated, an increasing significant correlation was observed between the markers for the OL and PVL groups. **Table 3** shows a summary of the results obtained in the linear regression and the equations for calculating the proportions of each related variable in each group. These results show through a mathematical model that the number of CD3 cells is explained by 84% of a CD8 population in the PVL group for this study ($P<0.0001$; $R^{2'}= 0.84$).

The levels of IL-5, IL-1β, and IFN-γ are differently expressed between OL and PVL

To assess the levels of cytokines and chemokines differentially expressed in the OL, PVL, and controls (IFH and OSCC) groups, initially, an analysis of variance was performed to identify which medians (cytokines) between the levels (groups) differed significantly. After evaluating the results obtained in the analysis of variance, it was observed that there was no difference between the medians within the groups studied for the cytokines IL-10, IL-12p70, IL-13, IL-17A, IL-21, IL-27, Granzyme A, Perforin, MIP-1β and sFasL.

The medians of the concentrations (pg/mL) of the cytokines that revealed different distribution between the groups were submitted to a multiple comparison test (**Figure 3**).

The results of this study showed that PVL when compared to the IFH group (a non-neoplastic inflammatory process), has increased levels of IL-2, IL-5, IL-23, and TNF-α. On the other hand, there was a reduction in the levels of several cytokines in the PVL group in relation to IFH and OSCC including IL-1β, IL-4, Il-6, IL-9, IL-18, IL-22, IFN-γ, GM-CSF, sCD137, granzyme B, sFAS, and MIP-1β. Additionally, few differences were found in the PVL group in relation to the

OL group, with only an increase in IL-5 and a reduction in IL-1β and IFN-γ in the first group. Evaluating the profile of the cytokines present in the protein extract of dysplastic OL samples, only an increase in IFN-γ and a reduction in IL-6 were identified in this group in relation to OSCC. On the other hand, a reduction in sCD-137, granzyme B, and MIP-1β was identified in the OL in relation to the IFH group.

No associations were observed between cytokine levels and the number of CD4 and CD8 cells for the OL group. However, the results of this study revealed a significant and regular inverse correlation between the number of CD4 cells and IL-22 levels (P=0.001; r=-0.56; R2=32%) for the PVL group, indicating that increased levels of IL-22 may be associated with a reduction in the number of CD4 cells in this group. When the number of CD8 cells and the levels of inflammatory cytokines in the PVL group were compared, a significant and regular correlation was observed for the levels of sCD137 (P=0.01; r=0.49) and MIP-1β (P=0.02; r=0.45). In addition, a significant and strong correlation was identified between CD8 cells and the cytokines GM-CSF (P<0.0001; r = 0.71), IFN-γ (P<0.0001; r = 0.70), TNF-α (P<0.0001; r = 0.72), IL-2 (P=0.0003; r = 0.68), IL-4 (P<0.0001; r = 0.71) , IL-5 (P<0.0001; r = 0.71), IL-6 (P<0.0001; r = 0.74), IL-10 (P<0.0001; r = 0.76) and IL-13 (P<0.0001; r = 0.74) for the PVL group. **Tables 4 and 5** show the results of the correlation between CD4 and CD8 cells, respectively, with the levels of inflammatory cytokines in OL and PVL samples. All the cytokines and chemokines levels included in the study are presented in **Supplementary 2**.

The conditioned medium from dysplastic keratinocytes derived from PVL patients may contribute to the Th17/Treg immune imbalance.

In order to complement the results found in the first stage of this study, the CM from normal (NOK), dysplastic (DOK and DOK-PVL), or neoplastic (SCC-25) keratinocytes were placed in contact with PBMC to evaluate whether factors released by these keratinocytes can modulate the Th phenotype (Th1, Th2, Th17, and Treg) and apoptosis rates of PBMC.

Performing a general assessment of the relative quantity of PBMC expressing the explored markers after the CM exposure, it can be observed that there is a predominance of CD4+ IFN-γ+ cells (for Th1) in all the CM groups tested. Statistical analysis of the data showed that CD4+ IL-IL-4+

population (for Th2) was significantly reduced in the PBMC exposed to RPMI (not stimulated group) and DOK-PVL CM in relation to the SCC-25 CM group (1.000±1.000 vs 1.705±4.018, *P*=0,0054 and 0.748±1.351 vs 1.705±4.018, *P*=0,0037, **Figure 4a**). Based on the relative quantity of IFN-γ+, IL-4+, IL-17A+ and FoxP3+ population, we calculated the IFN-γ+/IL-4+ (Th1/Th2) and IL-17A+/FoxP3+ (Th17/Treg) ratio in each CM group. Further analysis found that the $Th1/Th2_{PVL\text{-}CM}$ ratio was significantly higher than the $Th1/Th2_{RPMI\text{-}CM}$ ratio (1.160±3.945 vs 1.000±1.000, *P*=0,0061). Furthermore, the $Th17/Treg_{PVL\text{-}CM}$ ratio exhibited the opposite result comparing to $Th17/Treg_{RPMI}$ (0.152±0.411 vs 1.000±1.000, *P*=0,0013) and $Th17/Treg_{DOK\text{-}CM}$ (0.152±0.411 vs 0.391±1.321, *P*=0,021). These results may be observed in **Figure 4b**.

Apoptosis rates revealed that the soluble products contained in the CM derived from DOK-PVL and SCC-25 cell lines were able to significantly inhibit the apoptosis of PBMC, in relation to the CM derived from HOK cell line (0.341±0.525 vs 1.719±2.287, *P* =0.044 and 0.319±0.399 vs 1.719±2.287, *P*=0.032; respectively, **Figure 4c and 4d**).

DISCUSSION

Classification system for grading oral epithelial dysplasia proposed by WHO is commonly used by oral pathologists to indicate lesions that have a statistically higher risk of malignant transformation. However, this classification system is not completely accurate and reveals a large intra- and inter-examiner variability.[1,3,6] Within this paradigm, OL and PVL are two OPMDs that share similar microscopic characteristics but present distinct malignant transformation potential. The characterization of the inflammatory infiltrate in these two OPMDs may contribute to the elucidation of the different clinical behavior between them.

In the present study, it was demonstrated that dysplastic lesions of OL and PVL present quantitative changes in the inflammatory infiltrate mediated by T cells and a distinct cytokine profile. Initially, an increase in CD8 T cells present in the PVL group was demonstrated, as well as a higher density of these cells can be considered a risk factor for high-risk dysplasia. In addition, an increase in the number of CD8 T cells in human tumors has been associated with a favorable clinical prognosis. However, their precise function in the tumor microenvironment has not yet been clarified and their presence and effectiveness are rarely curative without manipulation.[27,28] In fact, CD8 T cells are central components of adaptive immunity against tumors. Effectors CD8 T cells

kill target cells and secrete cytokines that help stem the spread of pathogens and/or cancer. During antigen clearance, most effector CD8 T cells die from apoptosis, but about 5 to 10% survive and differentiate into memory CD8 T cells. Memory CD8 T cells are maintained for a long time in the absence of antigens and can exert rapid effector functions in response to previously identified antigens.[29-32] When host immune responses fail and antigens persist, antigen-specific CD8 T cells differentiate into a state called "exhaustion" and its showed reduced effective function and low proliferative capacity compared to CD8 T cells from functional memory.[33,34] Exhausted CD8 T cells have unique transcriptional and epigenetic signatures that may lead to functional and phenotypic changes. These cells demonstrate a reduction in several inflammatory cytokines and sequential loss of tumor necrosis factor-α (TNFα), interferon-γ (IFNγ), and cytotoxicity with an increased expression of multiple inhibitory receptors such as PD-1.[29,35-7] In this context, a recent study showed that PD-L1 immunoexpression in tumor cells and stromal cells were inversely correlated to CD8 T cells in OL and OSCC samples, similar to that found in other tumors such as pancreatic tumors.[38, 39] The authors of these studies suggest that the PD-1/PD-L1 pathway may be an important regulator of human oral carcinogenesis.

In addition, blocking PD-L1 promoted the infiltration of CD8 cells into the tumor and activation of the local immune response.[39] Data in the literature showed that PD-L1 is implicated in the immune escape of the tumor, inducing apoptosis in CD8 cells .[28, 40] Pre-existing CD8 T cells located on the tumoral front are associated with the expression of the PD-1/PD-L1 inhibitory pathway and represent a predictor of response to treatment.[41] Thus, it has been proposed that suppression of anti-tumor immunity by the PD-1/PD-L1 pathway in the OL can cause progression from the equilibrium phase to the escape phase, causing malignant transformation.[38] On the other hand, the concept of immuno-editing may explain the spontaneous cure of OL in some cases, as a process of reverse transformation from the equilibrium phase to the elimination phase when the immune system regains its protective function, detecting and destroying dysplastic cells.[17 , 18, 42, 43]

The complete activation of T cells occurs due to three signals; interaction between the antigenic peptide through MHC with TCR receptors, co-stimulation or co-inhibition using antigen-presenting cells, and the third signal characterized by the stimulation of extracellular cytokines such as IL-2.[44] Among these signals, the second determines the promotion or inhibition of T cell-related cytokines favoring or not the effector function of these cells.[41] Thus, one of the aspects of T cell immune exhaustion would be the production of effector chemokines stimulating an

insufficient immune response when related to the number of T cells.[46] In the present study we observed a low production of IL-1β, IL-4, IL-6, IL-9, IL-18, IL-22, IFN-γ, and GM-CSF for the PVL group when compared to the other study groups, as well as a large production of IL-2 and IL-5 which are two cytokines naturally produced by T cells and which act in the production of T and B lymphocytes, monocytes, natural killer cells, and eosinophils.[47, 48] Correlating the levels of chemokines with an increased number of CD8 T cells in the PVL group and the findings of the in vitro study demonstrating that CM derived from DOK-PVL and SCC-25 cell cultures are able to block the apoptosis index of PBMC, it may be assumed that dysplastic PVL lesions show a phenomenon of immunological exhaustion of CD8 T cells.

In the literature has been demonstrated that Th1 and Th17 cells have a pro-inflammatory function, whereas Th2 and Tregs cells modulate the immune tolerance, exhibiting an antagonist function.[49, 50, 51] Furthermore, the balance between Th1/Th2 and Th17/Tregs cells is fundamental for the maintenance of immunologic functions, and its imbalance can lead to chronic inflammation, uncontrolled cell proliferation, and finally carcinogenesis. In this context, we demonstrated that the soluble products produced by different keratinocytes cells were capable to modulate distinctly the Th phenotype. This was mainly evidenced after the analysis of the ratio Th1/Th2 and Treg/Th17 in DOK-PVL and SCC-25 MC. The imbalance of Treg/Th17 observed in DOK-PVL was similar to the observed for SCC-25, indicating that this could be an important factor to explain the high malignant transformation rate observed in PVL when compared to OL. The Treg/Th17 imbalance has already been demonstrated in several types of solid tumors, including colon, bladder, breast, and mouth carcinomas.[50-53] However, the studies published in the English literature regarding the participation of Th17 lymphocytes in carcinogenesis are quite controversial and some previous studies show that higher IL-17 expression is associated with a worse prognosis in head and neck SCC.[54] Accompanying this change in the Th17 population, an increase in Treg cells is associated with worse prognosis in head and neck SCC.[55-57] Additionally, it has been shown that there is a higher prevalence of these circulating subtypes of Th17 cells in patients with late-stage laryngeal and oropharyngeal tumors compared to patients with early stages.[58] Furthermore, an in vitro study using co-culture of PBMC with liver cancer cells showed that immune cells induce tumor cells to produce soluble factors capable of favoring the immunosuppressive response led by an increase in the Treg population in the tumor microenvironment.[59] It is important to notice that the proportion of Th17/Treg in the tumor microenvironment may influence tumor progression.

Studying the imbalance between these Th subtypes may help clarify the process of malignant transformation in OPMDs and tumor progression. In addition to the Treg / Th17 imbalance, the tumor microenvironment has a complex network of immune cells, including other lymphocytes subtypes such as Th1 and Th2 cells. Th2 cells secrete IL4, IL5, IL6, IL10, and IL13 which mediate the anti-inflammatory humoral response and immune suppression by inhibiting Th1 cytokine production, such as IFN-alpha, which are classified as pro-inflammatory and generally associated with a good prognosis.[50] In this regard, serum levels of IL-17A, TGF-β1, IL-4, and IL-10 were significantly higher in patients with OSCC, whereas IL-2 and IFN-γ were relatively low in OSCC patients compared with controls.[60] Apart from the expected, this study showed a reduction of CD4+IL-4+ population induced from DOK-PVL derivated MC compared to RPMI and SCC-25 groups. This was followed by an increase in the Th1/Th2 ratio in the DOK-PVL group. On the other hand, the high density of CD8+ T cells, the imbalance of Th17/Threg, and the cytokines profile observed in the PVL group appear to be more relevant for the malignant transformation rate in this OPMD compared to OL.

Cancer immunotherapy aims to restore the balance of dominant anti-tumor immunity through strategies such as vaccination with tumor antigens, blocking immunosuppressive signaling pathways, and adoptive cell therapy, among others. These approaches have produced significant responses in small subsets of patients with solid tumors, especially those with melanoma. It is important to note that the subset of patients who respond to therapies with vaccination and blocking immunosuppressive signaling pathways are those with an increased number of CD8 T cells in the tumor before starting therapy.[27, 29, 35] Given the findings of this study and in the literature data, immunotherapy may be a viable therapeutic strategy in a patient with OPMD, specifically in PVL. However, the poor representation of CD8 T cells in some tumors may represent a fundamental obstacle to the success of immunotherapy, in addition to the well-established barrier to immunosuppression. Therefore, new strategies are still needed to improve function and extend the effectiveness of immunotherapies to a broader set of cancer patients.

In summary, dysplastic lesions of patients with PVL have a high density of subepithelial CD8 T cells in relation to dysplastic lesions of OL, however, this high density does not correlate with histological risk. Furthermore, we noted that the correlation between cytokine/chemokine levels and immunohistochemical staining for CD8 T cells in dysplastic PVL lesions, suggests that the immune exhaustion phenomenon of CD8 T cells may be related to the clinical behavior of

PVL. In addition, the immune imbalance of T lymphocytes subsets and the cytokines profile observed in the PVL group appear to be relevant for the malignant transformation rate in this OMPD compared to OL. Considering the concept of the three Es of cancer immunoediting—elimination, equilibrium, and escape – and a subsequent study that suggests that OPMD may be in the elimination phase, [15,17, 18] our data propose that PVL may be in a more advanced phase. It is worth pointing out that this study has limitations, the main one being the absence of in vitro functional studies with co-culture of PBMC and keratinocyte cells, as well as in vivo studies, which would validate the results found. Thus, further studies are necessary to confirm the role of these immune cells and their factors in the pathogenesis of PVL, since these may be possible therapeutic targets.

Acknowledgments

The authors thank the Financial support that was provided by the São Paulo Research Foundation (FAPESP 2017/01438-0; 2017/01798-7; 2017/17288-8; 2018/22236-0; 2018/04954-2), Coordenação de Aperfeiçoamento de Pessoal de Nível Superior - Brasil (CAPES) – Finance code 001 and National Council for Scientific and Technological Development CNPq (423945/2016-5).

Authors contribution

D. F., C. O. B. - Writing - original draft, Methodology, Investigation, Formal Analysis, Data curation; M. P. P. – Investigation, Methodology; M. R. B. – Investigation, Methodology; T. M. F. - Data curation; Formal analysis; Software; H. A. S. - Data curation and Formal analysis; R. M. C. – Methodology, Visualization; L. Y. A. - Methodology, Visualization, Formal Analysis; J. E. L. - Data curation and Formal analysis; A. B. - Conceptualization; Funding acquisition; Investigation; Project administration; Resources; Supervision; Writing - review & editing.

REFERENCE LIST

1. El-Naggar AK, Chan JKC, Grandis JR, Takata T, Slootweg PJ. Tumours of the oral cavity and mobile tongue. In: El-Naggar AK, Chan JKC, Grandis JR, Takata T, Slootweg PJ, editors. World Health Organization (WHO) classification of head and neck tumours. International Agency for Research on Cancer (IARC). 4th ed. Lyon: IARCPress, 2017; 105–115.
2. Sook-Bin Woo. Oral Epithelial Dysplasia and Premalignancy. Head Neck Pathol. 2019 Sep; 13(3): 423–439.
3. Ranganathan K, Kavitha L. Oral epithelial dysplasia: Classifications and clinical relevance in risk assessment of oral potentially malignant disorders. J Oral Maxillofac Pathol. 2019 Jan-Apr;23(1):19-27.
4. Tilakaratne WM, Jayasooriya PR, Jayasuriya NS, De Silva RK. Oral epithelial dysplasia: Causes, quantification, prognosis, and management challenges. Periodontol 2000. 2019;80(1):126-147.
5. Petti S. Pooled estimate of world leukoplakia prevalence: a systematic review. Oral Oncol. 2003; 39(8):770-80.
6. Villa A, Sonis S. Oral leukoplakia remains a challenging condition. Oral Dis. 2018 Mar;24(1-2):179-183.
7. Bagan J, Scully C, Jimenez Y, Martorell M. Proliferative verrucous leukoplakia: a concise update. Oral Dis. 2010;16(4):328-332.
8. Warnakulasuriya S, Ariyawardana A. Malignant transformation of oral leukoplakia: A systematic review of observational studies. J Oral Pathol Med. 2016;45:155–66.
9. Aguirre-Urizar JM, Lafuente-Ibáñez de Mendoza I, Warnakulasuriya S. Malignant transformation of oral leukoplakia: Systematic review and meta-analysis of the last 5 years. Oral Dis. 2021 Nov;27(8):1881-1895.
10. Bagan JV, Jimenez Y, Sanchis JM, Poveda R, Milian MA, Murillo J, et al. Proliferative verrucous leukoplakia: high incidence of gingival squamous cell carcinoma. J Oral Pathol Med. 2003 Aug;32(7):379-382.
11. Villa A, Woo SB. Leukoplakia-A Diagnostic and Management Algorithm. J Oral Maxillofac Surg. 2017 Apr;75(4):723-734.

12. Torrejon-Moya A, Jané-Salas E, López-López J. Clinical manifestations of oral proliferative verrucous leukoplakia: A systematic review. J Oral Pathol Med. 2020;49(5):404-408.
13. Ramos-García P, González-Moles MÁ, Mello FW, Bagan JV, Warnakulasuriya S. Malignant transformation of oral proliferative verrucous leukoplakia: A systematic review and meta-analysis. Oral Dis. 2021 Nov;27(8):1896-1907.
14. Lafuente Ibáñez de Mendoza I, Lorenzo Pouso AI, Aguirre Urízar JM, Barba Montero C, Blanco Carrión A, Gándara Vila P, Pérez Sayáns M. Malignant development of proliferative verrucous/multifocal leukoplakia: A critical systematic review, meta-analysis and proposal of diagnostic criteria. J Oral Pathol Med. 2022 Jan;51(1):30-38. doi: 10.1111/jop.13246. Epub 2021 Oct 13. PMID: 34558734
15. Zitvogel L, Tesniere A, Kroemer G. Cancer despite immunosurveillance: immunoselection and immunosubversion. Nat Rev Immunol. 2006; 6:715-727.
16. Ai R, Tao Y, Hao Y, Jiang L, Dan H, Ji N, Zeng X, Zhou Y, Chen Q. Microenvironmental regulation of the progression of oral potentially malignant disorders towards malignancy. Oncotarget. 2017 Aug 17;8(46):81617-81635. doi: 10.18632/oncotarget.20312. PMID: 29113419; PMCID: PMC5655314.
17. aDunn GP, Old LJ, Schreiber RD. The three Es of cancer immunoediting. Annu Rev Immunol. 2004;22:329-360.
18. bDunn GP, Old LJ, Schreiber RD. The immunobiology of cancer immunosurveillance and immunoediting. Immunity. 2004;21(2):137-48.
19. Smyth MJ, Dunn GP, Schreiber RD. Cancer immunosurveillance and immunoediting: the roles of immunity in suppressing tumor development and shaping tumor immunogenicity. Adv Immunol. 2006;90:1-50.
20. Hanahan D, Weinberg RA. Hallmarks of cancer: the next generation. Cell. 2011; 144:646-674.
21. Vesely MD, Kershaw MH, Schreiber RD, Smyth MJ. Natural innate and adaptive immunity to cancer. Annu Rev Immunol. 2011;29:235-271.
22. Brouns E, Baart J, Karagozoglu K, Aartman I, Bloemena E, van der Waal I. Malignant transformation of oral leukoplakia in a well-defined cohort of 144 patients. Oral Dis. 2014;20:e19–e24.

23. Kujan O, Oliver RJ, Khattab A, Roberts SA, Thakker N and Sloan P: Evaluation of a new binary system of grading oral epithelial dysplasia for prediction of malignant transformation. Oral Oncol 2006, 42: 987-993.
24. Warnakulasuriya S, Reibel J, Bouquot J, Dabelsteen E. Oral epitelial dysplasia classification systems: predictive value, utility, weaknesses and scope for improvement. J Oral Pathol Med. 2008 Mar;37(3):127-133.
25. Tilakaratne WM, Jayasooriya PR, Jayasuriya NS, De Silva RK. Oral epithelial dysplasia: Causes, quantification, prognosis, and management challenges. Periodontol 2000. 2019; 80:126-147.
26. Basso FG, Pansani TN, Soares DG, Hebling J, de Souza Costa CA. LLLT Effects on Oral Keratinocytes in an Organotypic 3D Model. Photochem Photobiol. 2018 Jan;94(1):190-194
27. Peske JD, Woods AB, Engelhard VH. Control of CD8 T-Cell Infiltration into Tumors by Vasculature and Microenvironment. Adv Cancer Res. 2015; 128:263-307.
28. Yagyuu T, Hatakeyama K, Imada M, Kurihara M, Matsusue Y, Yamamoto K, Obayashi C, Kirita T. Programmed death ligand 1 (PD-L1) expression and tumor microenvironment: Implications for patients with oral precancerous lesions. Oral Oncol. 2017; 68:36-43.
29. Wherry EJ, Kurachi M. Molecular and cellular insights into T cell exhaustion. Nat Rev Immunol. 2015; 15:486-499.
30. Hashimoto M, Kamphorst AO, Im SJ, Kissick HT, Pillai RN, Ramalingam SS, Araki K, Ahmed R. CD8 T Cell Exhaustion in Chronic Infection and Cancer: Opportunities for Interventions. Annu Rev Med. 2018; 69:301-318.
31. Iwahori K. Cytotoxic $CD8^+$ Lymphocytes in the Tumor Microenvironment. Adv Exp Med Biol. 2020; 1224:53-62.
32. Williams MA, Bevan MJ. Effector and memory CTL differentiation. Annu Rev Immunol. 2007; 25:171-192.
33. Moskophidis D, Lechner F, Pircher H, Zinkernagel RM. Virus persistence in acutely infected immunocompetent mice by exhaustion of antiviral cytotoxic effector T cells. Nature. 1993; 362:758-761.

34. Zajac AJ, Blattman JN, Murali-Krishna K, Sourdive DJ, Suresh M, Altman JD, Ahmed R. Viral immune evasion due to persistence of activated T cells without effector function. J Exp Med. 1998; 188:2205-2213.

35. Wherry EJ, Ha SJ, Kaech SM, Haining WN, Sarkar S, Kalia V, Subramaniam S, Blattman JN, Barber DL, Ahmed R. Molecular signature of CD8+ T cell exhaustion during chronic viral infection. Immunity. 2007; 27:670-684.

36. Sen DR, Kaminski J, Barnitz RA, Kurachi M, Gerdemann U, Yates KB, Tsao HW, Godec J, LaFleur MW, Brown FD, Tonnerre P, Chung RT, Tully DC, Allen TM, Frahm N, Lauer GM, Wherry EJ, Yosef N, Haining WN. The epigenetic landscape of T cell exhaustion. Science. 2016; 354:1165-1169.

37. Barber DL, Wherry EJ, Masopust D, Zhu B, Allison JP, Sharpe AH, Freeman GJ, Ahmed R. Restoring function in exhausted CD8 T cells during chronic viral infection. Nature. 2006; 439:682-687.

38. Stasikowska-Kanicka O, Wągrowska-Danilewicz M, Danilewicz M. CD8+ and CD163+ infiltrating cells and PD-L1 immunoexpression in oral leukoplakia and oral carcinoma. APMIS. 2018; 126:732-738.

39. Nomi T, Sho M, Akahori T, Hamada K, Kubo A, Kanehiro H, Nakamura S, Enomoto K, Yagita H, Azuma M, Nakajima Y. Clinical significance and therapeutic potential of the programmed death-1 ligand/programmed death-1 pathway in human pancreatic cancer. Clin Cancer Res. 2007; 13:2151-2157.

40. Qian BZ, Pollard JW. Macrophage diversity enhances tumor progression and metastasis. Cell. 2010; 141:39-51.

41. Maj T, Wei S, Welling T, Zou W. T cells and costimulation in cancer. Cancer J. 2013 Nov-Dec;19(6):473-482.

42. Kuribayashi Y, Tsushima F, Morita KI, Matsumoto K, Sakurai J, Uesugi A, Sato K, Oda S, Sakamoto K, Harada H. Long-term outcome of non-surgical treatment in patients with oral leukoplakia. Oral Oncol. 2015; 51:1020-1025.

43. Mittal D, Gubin MM, Schreiber RD, Smyth MJ. New insights into cancer immunoediting and its three component phases--elimination, equilibrium and escape. Curr Opin Immunol. 2014; 27:16-25.

44. Murakami N, Riella LV. Co-inhibitory pathways and their importance in immune regulation. Transplantation. 2014; 98:3-14.
45. Maj T, Wei S, Welling T, Zou W. T cells and costimulation in cancer. Cancer J. 2013 Nov-Dec;19(6):473-482.
46. Pauken KE, Wherry EJ. Overcoming T cell exhaustion in infection and cancer. Trends Immunol. 2015 Apr;36(4):265-276.
47. McDermott DF, Regan MM, Atkins MB. Interleukin-2 therapy of metastatic renal cell carcinoma: update of phase III trials. Clin Genitourin Cancer. 2006 Sep;5(2):114-119.
48. Dougan M, Dranoff G, Dougan SK. GM-CSF, IL-3, and IL-5 Family of Cytokines: Regulators of Inflammation. Immunity. 2019 Apr 16;50(4):796-811.
49. Murugaiyan G, Saha B. Protumor vs antitumor functions of IL-17. J Immunol. 2009;183(7):4169-75.
50. Gaur P, Singh AK, Shukla NK, Das SN. Inter-relation of Th1, Th2, Th17 and Treg cytokines in oral cancer patients and their clinical significance. Hum Immunol. 2014;75(4):330-7.
51. Mougiakakos D, Choudhury A, Lladser A, Kiessling R, Johansson CC. Regulatory T cells in cancer. Adv Cancer Res. 2010;107:57-117.
52. Duan MC, Zhong XN, Liu GN, Wei JR. The Treg/Th17 paradigm in lung cancer. J Immunol Res. 2014; 2014:730380.
53. Chi LJ, Lu HT, Li GL, Wang XM, Su Y, Xu WH, Shen BZ. Involvement of T helper type 17 and regulatory T cell activity in tumour immunology of bladder carcinoma. Clin Exp Immunol. 2010 Sep;161(3):480-9.
54. Kesselring R, Thiel A, Pries R, Wollenberg B. The number of CD161 positiveTh17 cells are decreased in head and neck cancer patients. Cell Immunol. 2011;269(2):74-7.
55. Strauss L, Bergmann C, Gooding W, Johnson JT, Whiteside TL. The frequency and suppressor function of CD4+CD25highFoxp3+ T cells in the circulation of patients with squamous cell carcinoma of the head and neck. Clin Cancer Res. 2007;13(21):6301-11.
56. Drennan S, Stafford ND, Greenman J, Green VL. Increased frequency and suppressive activity of CD127(low/-) regulatory T cells in the peripheral circulation of patients with

head and neck squamous cell carcinoma are associated with advanced stage and nodal involvement. Immunology. 2013;140(3):335-43.

57. Sun W, Li WJ, Wu CY, Zhong H, Wen WP. CD45RA-Foxp3high but not CD45RA+Foxp3low suppressive T regulatory cells increased in the peripheral circulation of patients with head and neck squamous cell carcinoma and correlated with tumor progression. J Exp Clin Cancer Res. 2014;33:35.

58. Green VL, Michno A, Stafford ND, Greenman J. Increased prevalence of tumour infiltrating immune cells in oropharyngeal tumours in comparison to other subsites: relationship to peripheral immunity. Cancer Immunol Immunother. 2013 May;62(5):863-73.

59. Zhao Q, Wang PP, Huang ZL, Peng L, Lin C, Gao Z, Su S. Tumoral indoleamine 2,3-dioxygenase 1 is regulated by monocytes and T lymphocytes collaboration in hepatocellular carcinoma. Oncotarget. 2016 Mar 22;7(12):14781-90.

60. Dutta A, Banerjee A, Saikia N, Phookan J, Baruah MN, Baruah S. Negative regulation of natural killer cell in tumor tissue and peripheral blood of oral squamous cell carcinoma. Cytokine. 2015 Dec;76(2):123-130.

TABLES

Table 1 – Clinicopathological characteristics of OL and PVL patients.

Parameters		OL N=19	PVL N=12	*p-value*
		n (%)	n (%)	
Age				
	Average years	52.2	64.3	0.01
Sex				
	Male	11 (57.9)	6 (50.0)	0.66
	Female	8 (42.1)	6 (50.0)	
Race				
	White	15 (78.9)	12 (100.0)	0.13
	Non-white	4 (21.1)	0 (0.0)	
Tobacco				
	No	9 (47.4)	8 (66.7)	0.46
	Yes	10 (52.6)	4 (33.3)	
Alcohol				
	No	18 (94.7)	10 (83.3)	0.54
	Yes	1 (5.3)	2 (16.7)	
Total lesion size				
	Less than 3 cm	16 (84.2)	0 (0.0)	<0.0001
	Larger than 3 cm	3 (15.8)	12 (100.0)	
Spreading				
	No	19 (100.0)	0 (0.0)	<0.0001
	Yes	0 (0.0)	12 (100.0)	
Histopathological risk				
	Low risk	13 (68.4)	16 (59.3) $^{++}$	0.52
	High risk	6 (31.6)	11 (40.7) $^{++}$	
Malignant transformation				
	No	16 (84.2)	5 (41.7)	0.02
	Yes	3 (15.8)	7 (58.3)	
Recurrence				
	No	19 (100.0)	3 (25.0)	<0.0001
	Yes	0 (0.0)	9 (75.0)	

$^{++}$ Number of events considering the number of paraffin samples (n=27) obtained from the PVL group (n=12).
P *value* ≤0.05 indicates a statistically significant difference.

Table 2. Logistic regression results relating the risk of dysplasia in OL and PVL according to lymphocytes markers.

		Model Coefficients			Categorial Variable Results		
Group	**Marker**	**-2 Log likelihood**	**Chi-square**	**p-value**	**p-value**	**Odds ratio**	**CI 95%**
OL	CD3	29.435	0.2847	0.5936	0.5922	1.6500	0.26 – 10.31
	CD4	29.435	0.2847	0.5936	0.5922	1.6500	0.26 – 10.31
	CD8	27.908	1.8119	0.1783	0.1872	3.3333	0.59 – 19.95
PVL	CD3	39.676	0.2277	0.6332	0.6737	1.4667	0.30 – 7.19
	CD4	38.684	1.2193	0.2695	0.2921	2.5667	0.44 – 14.82
	CD8	**35.892**	**4.0112**	**0.0450**	**0.0452**	**6.8571**	**0.75 – 62.96**

OL: oral leukoplakia; PVL: proliferative verrucous leukoplakia; CI: Confidence interval; P-value ≤0.05 indicates a statistically significant difference.

Table 3. Summary of simple linear regression for CD4 and CD8 markers in OL and PVL groups.

Group	Y	X	*p*-value	$R^{2'}$	*p*-value (a)	*p*-value (b)	Equation log Y = a + b. log X	95% CI (a)	95% CI (b)
OL	CD3	CD4	<0.0001	0.94	<0.0001	<0.0001	log Y = 0.41 + 0.85 log X	0.26 - 0.56	0.75 - 0.95
	CD3	CD8	<0.0001	0.87	0.10	<0.0001	log Y = 0.21 + 1.20 log X	-0.05 - 0.58	0.98 - 1.42
	CD4	CD8	<0.0001	0.87	0.23	<0.0001	log Y = -0.18 + 1.37 log X	-0.49 - 0.13	1.11 - 1.62
	CD8	CD4	<0.0001	0.87	0.01	<0.0001	log Y = 0.25 + 0.64 log X	0.06 - 0.43	0.52 - 0.76
PVL	CD3	CD4	0.0015	0.31	<0.0001	0.0011	log Y = 1.26 + 0.64 log X	0.77 - 1.76	0.28 - 1.00
	CD3	CD8	<0.0001	0.84	<0.0001	<0.0001	log Y = 0.86 + 0.81 log X	0.63 - 1.12	0.67 - 0.95
	CD4	CD8	<0.0001	0.57	0.26	<0.0001	log Y = 0.20 + 0.67 log X	-0.17 - 0.58	0.49 - 0.90
	CD8	CD4	<0.0001	0.57	0.04	<0.0001	log Y =0 .42 + 0.87 log X	0.01 - 0.82	0.58 - 1.16

Y: dependent variable; X: independent variable; $R^{2'}$: Adjusted coefficient of determination; (a): linear coefficient; (b): angular coefficient; 95% CI: confidence interval. P *value* ≤0.05 indicates a statistically significant difference.

Table 4 - Spearman correlation between CD4 immunohistochemical expression and cytokine and chemokine levels of dysplastic lesions of OL and PVL groups.

	OL			PVL		
	p-value	R	R^2 (%)	*p-value*	R	R^2 (%)
GM-CSF	0.75	0.06	0.4	0.25	0.22	4.9
IFN-γ	0.84	0.04	0.1	0.25	0.22	4.9
TNF-α	0.72	0.07	0.5	0.27	0.21	4.4
IL-10	0.85	0.04	0.1	0.18	0.25	6.7
IL-12p70	0.87	0.03	0.1	0.22	0.23	5.6
IL-13	0.39	-0.18	0.03	0.35	0.20	4.0
IL-17A	0.80	0.05	0.2	0.28	0.20	4.3
IL-18	0.84	0.04	0.1	0.23	0.23	5.6
IL-1β	0.88	0.03	0.09	0.22	0.23	5.6
IL-2	0.63	-0.1	1.0	0.35	0.18	3.2
IL-21	0.84	0.04	0.1	0.18	0.25	6.6
IL-22	0.85	0.04	0.1	**0.001**	**-0.56**	**32.1**
IL-23	0.62	0.1	1.1	0.21	0.24	5.8
IL-27	0.79	0.05	0.3	0.24	0.22	5.2
IL-4	0.86	0.03	0.1	0.25	0.22	4.9
IL-5	0.61	-0.1	1.1	0.28	0.20	4.3
IL-6	0.90	0.02	0.07	0.22	0.23	5.6
IL-9	0.87	0.03	0.1	0.28	0.20	4.4

r: Spearman correlation coefficient; R^2: Coefficient of determination expressed in %.
P *value* ≤0.05 indicates a statistically significant difference.

Table 5 - Spearman correlation between CD8 immunohistochemical expression and cytokine and chemokine levels of dysplastic lesions of OL and PVL groups.

	OL			PVL		
	p-value	R	R^2 (%)	*p-value*	R	R^2 (%)
GM-CSF	0.62	0.10	1.0	**<0.0001**	**0.72**	**52.2**
SCD137	0.38	0.21	4.4	**0.01**	**0.49**	**24.1**
IFN-γ	0.68	0.08	0.7	**<0.0001**	**0.70**	**50.3**
TNF-α	0.61	0.10	1.1	**<0.0001**	**0.72**	**52.2**
Perforin	0.41	-0.20	4.0	0.33	0.19	4.0
Granzyme A	0.42	-0.19	3.7	0.07	0.36	13.2
Granzyme B	0.41	0.20	4.0	0.07	0.36	13.1
IL-2	0.77	-0.06	0.3	**0.0002**	**0.68**	**46.9**
IL-4	0.71	0.07	0.6	**<0.0001**	**0.71**	**50.9**
IL-5	0.76	-0.06	0.4	**<0.0001**	**0.71**	**51.2**
IL-6	0.74	0.07	0.5	**<0.0001**	**0.74**	**55.7**
IL-10	0.69	0.08	0.7	**<0.0001**	**0.76**	**58.7**
IL-13	0.57	0.12	1.4	**<0.0001**	**0.74**	**54.8**
sFas	0.43	-0.18	3.5	0.08	0.35	12.6
sFasL	0.35	-0.22	5.1	0.33	0.20	4.0
MIP-1α	0.21	-0.30	9.0	0.73	-0.07	0.4
MIP-1β	0.33	0.23	5.5	**0.02**	**0.45**	**20.9**

r: Spearman correlation coefficient; R^2: Coefficient of determination expressed in %.
P *value* ≤0.05 indicates a statistically significant difference.

FIGURE LEGENDS LIST

Figure 1. Tissue fragments stained with H&E and the respective immunohistochemical staining patterns for CD3, CD4, and CD8 T cells observed in the OL and PVL groups (20X magnification).

Figure 2. The number of T lymphocytes associated with OL and PVL was identified by immunohistochemistry. Mean number of CD3, CD4, and CD8 cells counted in the intraepithelial and subepithelial areas.

Figure 3. Cytokines and chemokines profile in IFH, OL, PVL, and OSCC using the multiplex assay with frozen tissue samples. Average concentration (pg/mL) of cytokines and chemokines with significant statistical differences found between the studied groups. * $p < 0.05$.

Figure 4. Modulation of the Th1, Th2, Th17, and Treg phenotype and apoptosis rates in PBMC after contact with CM derived from HOK, DOK, DOK-PVL, and SCC-25. **(A)** Relative percentage of CD4+ IFN-γ+ cells (for Th1), CD4+ IL-4+ (for Th2), CD4+ IL-17A+ (for Th17), and CD4+ Foxp3+ (for Treg) for each condition tested. **(B)** Th1/Th2 and Th17/Treg ratio. **(C)** Representative graphics highlighting reduced apoptosis rates in the PBMC after contact with CM from DOK-PVL and SCC-25 in relation to the CM from HOK. **(D)** The average and standard deviation from each group. * $p < 0.05$ and ** $p < 0.01$.

Supplementary 1. Representative images of primary keratinocytes isolated from dysplastic lesion of proliferative verrucous leukoplakia (DOK-PVL) and normal human oral keratinocytes (HOK). View of keratinocytes DOK-PVL **(A)** and HOK **(C)** under the phase-contrast microscope. Immunofluorescence staining with antibody to human cytokeratin AE1/AE3 in DOK-PVL **(B)** and HOK **(D)** cell cultures. The primary DOK-PVL keratinocytes came from a leukoplastic lesion in a 76-year-old male patient diagnosed with PVL and a previous history of malignant transformation. The tissue fragment was collected from an area of the lower alveolar ridge showing a white plaque with a rough surface that microscopically revealed moderate epithelial dysplasia (high risk). After isolating the keratinocytes, colonies of cells composed of a mixture of polygonal cells and cells that reveal important cellular pleomorphism were observed. This population of mixed cells remained viable for a maximum of 5 passages and its epithelial origin was confirmed by immunofluorescence with antibody to human cytokeratin AE1/AE3. In order to obtain primary cultures of HOK, fragments of gingival tissue were collected from a 54-year-old male subject who underwent clinical crown augmentation surgery. HOK cell cultures characteristically revealed the formation of homogeneous polygonal cell colonies, their epithelial origin being confirmed by immunofluorescence with antibody to human cytokeratin AE1/AE3.

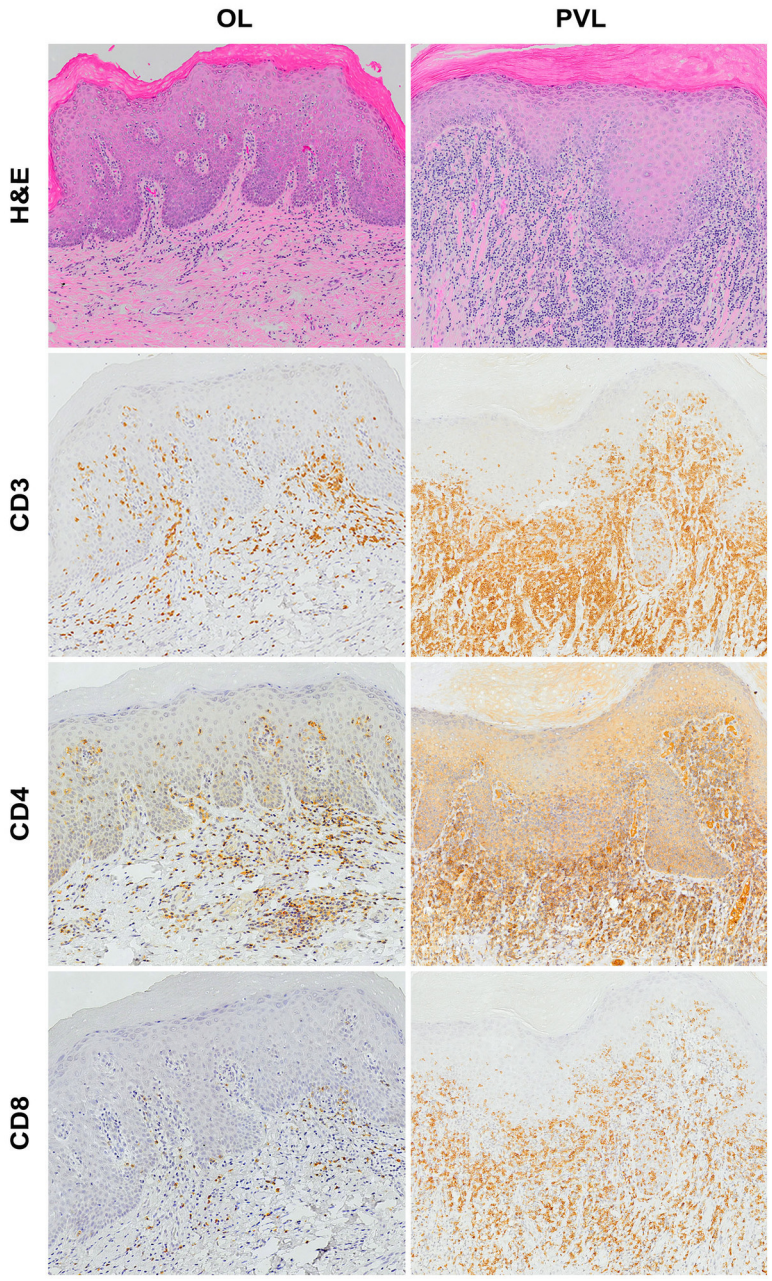

IMM_13565_Figure1.jpg

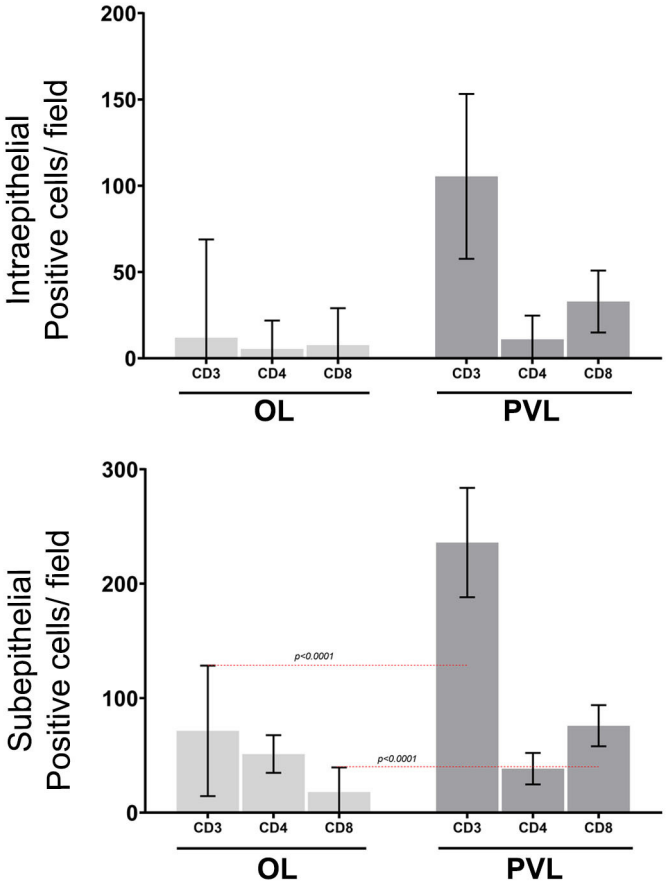

IMM_13565_Figure 2.jpg

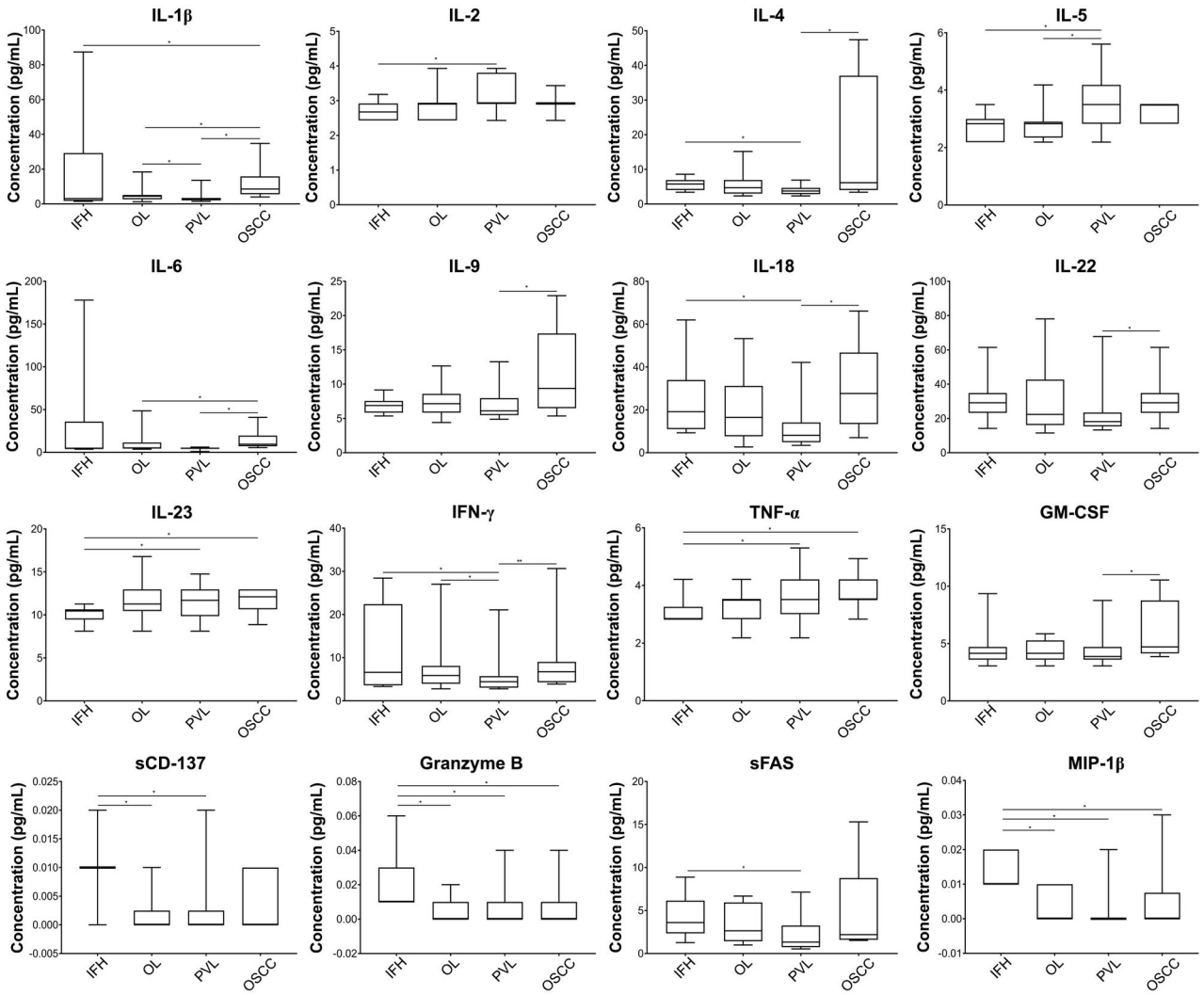

IMM_13565_Figure 3.jpg

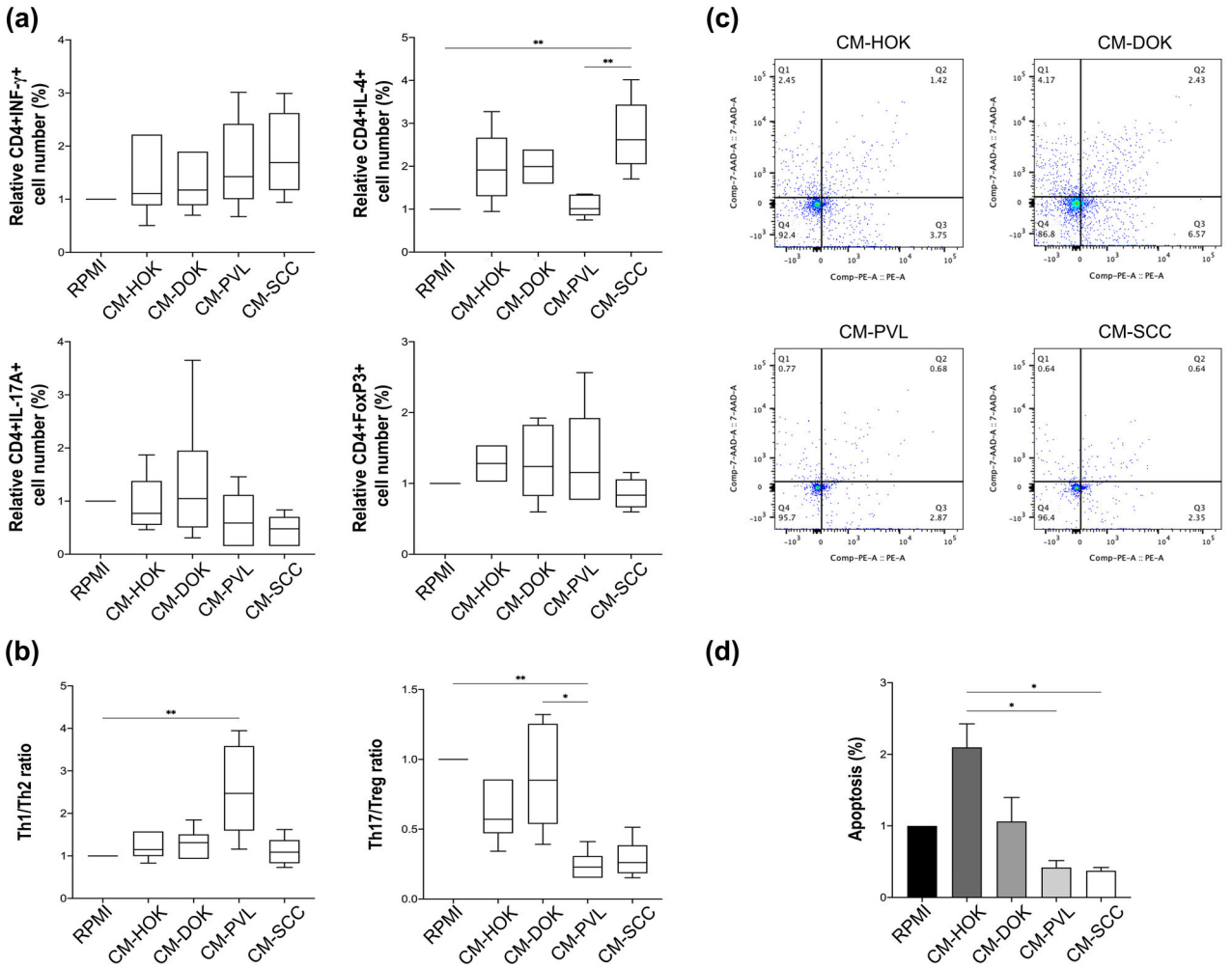

IMM_13565_Figure 4.jpg